25th ABCM International Congress of Mechanical Engineering
October 20-25, 2019, Uberlândia, MG, Brazil

COB-2019-2359
NUMERICAL ANALYSIS OF THE FLOW MULTI-PHASE IN A MANIFOLD: MODELING AND SIMULATION

Hortência Luma Fernandes Magalhães
Danielle de Lima Vieira
Guilherme Luiz de Oliveira Neto
Tony Herbert Freire de Andrade
Severino Rodrigues de Farias Neto
Federal University of Campina Grande, Campina Grande, Paraíba, Brazil.
hortencia.luma@gmail.com
danielle_ufcg@hotmail.com
guilherme@ifpi.edu.br
tonyhebert2000@gmail.com
s.fariasn@gmail.com

Jéssica Barbosa da Silva do Nascimento
State University of Santa Cruz, Ilhéus-Ba, Brazil.
nascimentojessicabarbosa@gmail.com

José Ricardo Ferreira Oliveira
Federal University of Uberlândia, Uberândia,Minas Gerais, Brazil.
jose.ricardo@ufu.br

Abstract. *Use of a manifold as a tool for conducting fluids (oil, water, gas) during oil extraction up until surface, has attracted the interest of researchers seeking to optimize oil production by combining the flow and pressure of several wells, in primary processing plants. In this sense, fluid flow dynamics (oil/water/gas) in a manifold were studied numerically. Manifold used consisted of the main branch connected to five perpendicular secondary branches, four pipes coming from the wells and one conduct to lead oil/water/gas streams to the primary processing sector. The mass conservation equations, linear momentum in conjunction with the standard RNG k-ε turbulence model were solved with the ANSYS CFX® 15, commercial package. The mixing model was used to treat conservation equations for the present phases (oil/water/ gas). Turbulent, isothermal flow and constant fluid properties were considered. Results, after analysis of the velocity fields, volumetric fraction and mass flow allowed the minimization of water production.*

Keywords*: Oil, manifold, computational fluid dynamics.*

1. INTRODUCTION

Petroleum plays an important role in world energy policy, noting that its utilization is not restricted to use as a fuel, but also meets the huge demand existent for its derivatives, for example, the plastics. According to Oliveira (2013), the oil reservoirs found under the seabed are produced through production underwater systems, which are composed of sets of equipment with specific purposes in the development of these reservoirs/oil fields.

During Offshore oil production, fluids (oil, water, gas) leaving the reservoir after drilling well will be conducted to the surface through lines production (risers). According to Thomas (2001), the system starts at the wellhead, which is equipped with a valve for flow control according to reservoir engineering recommendations. To optimize production, in the presence of two or more wells in the same unit, it is necessary to use a production manifold to combine the flows and pressures of several wells to the primary processing plant (Thomas, 2001).

Oil production is the main goal of the oil industry, so minimizing water production in the wells to maximize oil production is a challenge. For this, production tests are performed; mass flow analysis and production optimization proposals are continuously performed. A numerical simulation is a tool that has gained visibility in the industrial field by contributing to solutions to problems in which a laboratory experiment would be economically unfeasible, especially in situations where it is impossible to reproduce in laboratory benches.

In the petroleum industry, Computational Fluid Dynamics (CFD) is used in many cases to numerically represent the flow of fluids, mainly in pipes, and with this to understand the fluid dynamics of the process, making it possible to

obtain information such as: mass flow, pressure fields and velocity, volumetric fractions among other parameters. Therefore, the goal of this work is to present proposals for the minimization of water production in a manifold.

2. METHODOLOGY

2.1 Mesh building

The study domain evaluated corresponds to a hypothetical manifold, which allows the production flow of four oil wells in a sedimentary basin. The domain dimensions are the following Fig. (1). The numerical mesh was built in the ANSYS ICEM® Release 15.0 by the multi-block technique. The developed mesh has 300842 hexahedral elements and 284332 knots. Figures 2 and 2b show the domain and inlet wall of well 1, respectively.

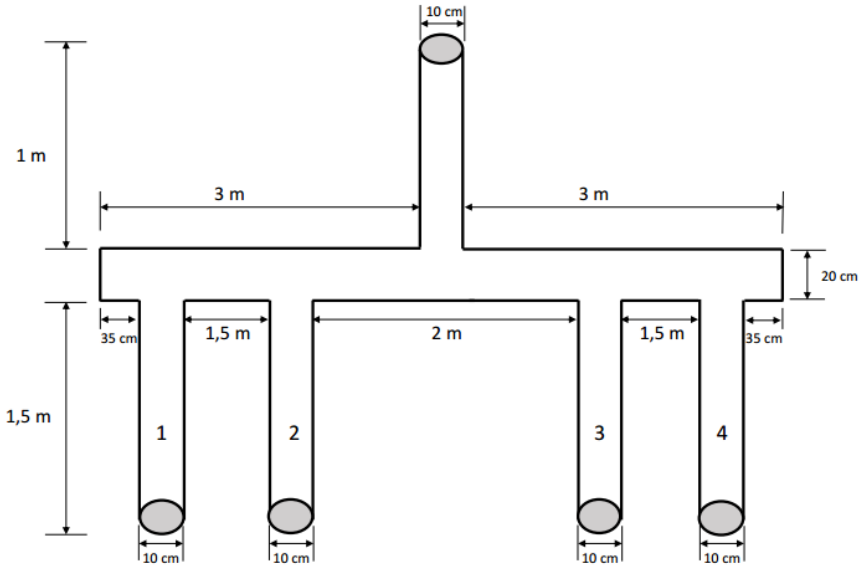

Figure 1. Manifold with four connected wells, representing the study domain.

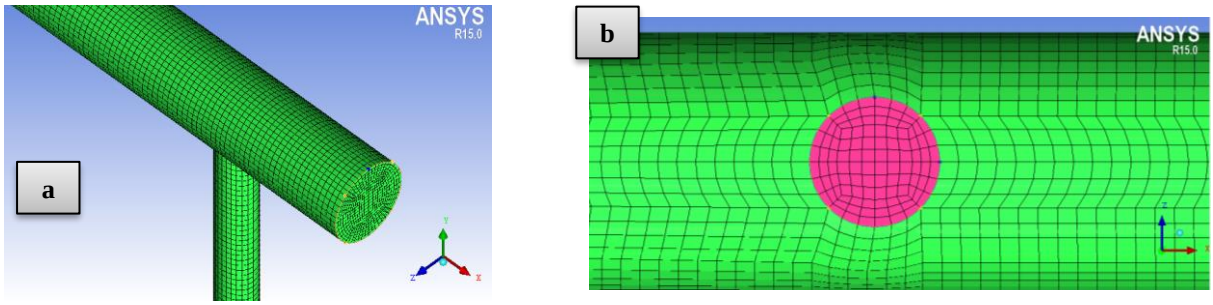

Figure 2. Numeric mesh showing (a) the domain wall and (b) inlet wall of well 1

2.2 Mathematical modeling

Mathematical modeling used was Eulerian-Eulerian, which is one of the two main multiphase models implemented in ANSYS CFX 15.0. Within the Eulerian-Eulerian model, the interfacial transfer terms were modeled using the non-homogeneous multiphase model, called the blending model. The turbulence model used for the three phases was the model RNG k- ε. Transport equations were used considering the following simplifications: isothermal flow, permanent and incompressible regime. As it is an isothermal flow, the energy equation was not used. For a steady-state, the transient terms of the conservation equations of mass and momentum are null. The term of interfacial mass transfer was not considered in the momentum equation (Araújo *et al.* 2014, Alves *et al.* 2016, Barbosa 2011). Equations of continuity (Eq. 1) and momentum (Eq. 2) are written, respectively, with the following simplifications:

$$\nabla \bullet (f_\alpha \rho_\alpha \overrightarrow{U_\alpha}) = 0 \qquad (1)$$

$$\nabla \bullet [f_\alpha(\rho_\alpha \overrightarrow{U_\alpha} \otimes \overrightarrow{U_\alpha})] = -f_\alpha \nabla P_{p_\alpha} + \nabla \bullet \{f_\alpha(\tau_\alpha + \tau_\alpha^{turb} + \tau_S)\} + \sum_{\beta-1}^{Np} (\Gamma^+_{\alpha\beta} \overrightarrow{U_\beta} - \Gamma^+_{\beta\alpha} \overrightarrow{U_\alpha}) \quad (2)$$

In the mixing model, only the drag exerted by phase β on phase α per unit volume is considered, where $D_{\alpha\beta}$ is defined by Eq. 3

$$D_{\alpha\beta} = C_D \rho_{\alpha\beta} A_{\alpha\beta} \left|\vec{U}_\beta - \vec{U}_\alpha\right| \left(\vec{U}_\beta - \vec{U}_\alpha\right) \quad (3)$$

In Equation 3, the C_D is the constant dimensionless drag coefficient, assumed to be 0.44. $\rho_{\alpha\beta}$ corresponds to the density of the mixture given by Eq. 4. Interfacial area density per unit volume, $A_{\alpha\beta}$, is given by Eq. 5.

$$\rho_{\alpha\beta} = f_\alpha \rho_\alpha + f_\beta \rho_\beta \quad (4)$$

$$A_{\alpha\beta} = \frac{f_\alpha f_\beta}{d_{\alpha\beta}} \quad (5)$$

The turbulence model chosen for all simulations is the standard k-ε model, which is classified as a model of two equations: the turbulent kinetic energy equation, k, and the turbulent dissipation rate equation, ε. It was chosen because it is one of the most notable models of turbulence and is considered the industry standard model (Araújo et al, 2014). The transport equations for estimating the variables, k, turbulent kinetic energy, ε, and the turbulent dissipation rate are given by Eq. 6 and 7.

$$\frac{\partial(\rho k)}{\partial t} + \frac{\partial}{\partial x_j}\left(\rho U_j k\right) = \frac{\partial}{\partial x_j}\left[\left(\mu + \frac{\mu_t}{\sigma_k}\right)\frac{\partial k}{\partial x_j}\right] + P_k - \rho\varepsilon + P_{kb} \quad (6)$$

$$\frac{\partial(\rho \varepsilon)}{\partial t} + \frac{\partial}{\partial x_j}\left(\rho U_j \varepsilon\right) = \frac{\partial}{\partial x_j}\left[\left(\mu + \frac{\mu_t}{\sigma_\varepsilon}\right)\frac{\partial \varepsilon}{\partial x_j}\right] + \frac{\varepsilon}{k}\left(C_{\varepsilon 1} P_k - C_{\varepsilon 2}\rho\varepsilon + C_{\varepsilon 1} P_{\varepsilon b}\right) \quad (7)$$

In these equations, we have C_{z1} and C_{z2} are empirical constants, respectively equal to 1.44 and 1.92; σ_z and σ_k are constants equal to 1.0 and 1.3 respectively. P_{kb} and P_{zb} represent the influence of buoyancy forces [4]. The term P_k, which appears in both equations, represents the portion of turbulent kinetic energy production defined by Barbosa, 2011, and is given by Eq. 8.

$$P_k = \mu_{ef} \nabla \vec{U}_\alpha \left[\nabla \vec{U}_\alpha + (\nabla \vec{U}_\alpha)^T\right] - \frac{2}{3}\nabla \vec{U}_\alpha \left(\mu_{eff} \nabla \vec{U}_\alpha + \rho k\right) \quad (8)$$

2.3 Boundary conditions

Proposal 1: At input 1, the velocity, U, was taken as 1.5 m/s; at inputs 2, 3 e 4 it was considered with boundary condition the mass flow rate (Q_m = 11.6514 kg/s), calculated to maintain the same flow rate of the well 1, using the expression: $Q_m = \left(\pi v_i D^2 / 2\rho_o\right)$ (Equation 1), where v_i is the velocity in inlet 1, D is the diameter of the inlet 1, and ρ_o is the density of the oil. At the outlet, a static pressure was considered (P_{est} = 98,69 atm). In the walls was considered the non-slip condition for the three phases, besides a value of 0.15 mm for the roughness.

Proposal 2: Input 1 was considered a velocity U equals 1.5 m/s, and at input 3 was maintained as an initial condition the mass flow calculated using Equation 1. At Input 2, was used Q_m = 8.6514 kg/s, and in input 4, Q_m = 14.6514 kg/s. At the output was considered a static pressure P_{est} = 98.6923 atm. In the walls was considered the non-slip condition for the three phases, besides a value of 0.15 mm for the roughness.

Proposal 3: At input 1, was considered a velocity U equals 1.5 m/s, at input 3 was assumed as the initial condition, the mass flow calculated using Equation 1. At input 2, it was considered, Q_m = 10.6514 kg/s and at inlet 4, Q_m = 12.6514 kg/s. At output was considered a pressure boundary condition (P_{est} = 98.6923 atm). In the walls was considered the non-slip condition for the three phases, besides a value of 0.15 mm for the roughness.

2.4 Fluid properties

Fluid properties are available in Tab. 1 and phase volume fractions are available in Tab. 2.

Table 1 - Fluid properties

Properties	Water	Oil	Air (25 ºC)
Density ($Kg.m^{-3}$)	989	997	1.85
Viscosity ($Kg.m^{-1}.s^{-1}$)	5	0.0008899	1.831×10^{-5}

Table 2. Volume fractions

Volume fractions	Well distribution			
	Well 1	Well 2	Well 3	Well 4
f_a	-	20%	-	10%
f_g	-	-	10%	10%
f_o	100 %	80%	90%	80%

3. RESULTS AND DISCUSSION

For the proposals 1, 2 and 3 the following results were obtained: oil phase volumetric fraction, velocity fields and predominant flow patterns.

3.1 Volumetric fraction

Figures (3), (4) and (5) show the oil phase volumetric fractions present in the flow of proposals 1, 2 and 3. It is observed the predominance of the oil phase over the other phases and its flow in the center of the pipeline in the three-phase flow regions (oil-water-gas), with an accumulation of the water phase in the lower part of the horizontal pipeline and preferential flow of the gas near the wall.

The oil and gas tend to flow together in the upper part of the duct due to the difference in density between the phases, thus confirming the influence of the gravitational force during the flow, with the formation of the stratified flow pattern, where the three phases involved flow separated by an interface. This same behavior is observed in the three proposals (Fig. 6, 7 and 8).

3.2 Velocity field

Figures (9), (10) and (11) shows the velocity field for all fluids (oil/gas/water), respectively. It can be observed that the velocity, for all fluids (water / oil / gas), is zero in the region of contact with the wall, increasing towards the duct center, where it reaches its maximum value, varying according to the changes in the pipe diameter to maintain the same mass flow at the inlet, since flow occurs in steady-state. In the region of abrupt change between the horizontal and vertical sections of exit, a considerable increase of velocity in the direction of the exit is observed (Silva *et al.* 2011). While in the horizontal section of the larger diameter, the lower velocity is observed. There are also small changes in the velocities of the phases as a function of the changes in the flows of the wells when comparing the three proposals. Similar behavior was observed in proposals 2 and 3.

3.3 Mass flow rate produced

Table 3 shows the mass flow rates obtained in the simulations performed on proposals 1, 2 and 3. The mass flow rates of the wells were assumed to minimize the water production, but maintaining the total flow at the manifold outlet. It is observed, therefore, that Proposal 3 presents the lowest water mass flow rate at the manifold outlet when compared with the data obtained from Proposals 1 and 2.

Table 3. Mass flows rate of phases at the manifold outlet.

Mass flows rate	Water ($kg\ s^{-1}$)	Gas ($kg\ s^{-1}$)	Oil ($kg\ s^{-1}$)
Proposal 1	3.64194	0.00310128	42.8245
Proposal 2	3.54795	0.00322734	42.9241
Proposal 3	3.35796	0.00350341	43.1054

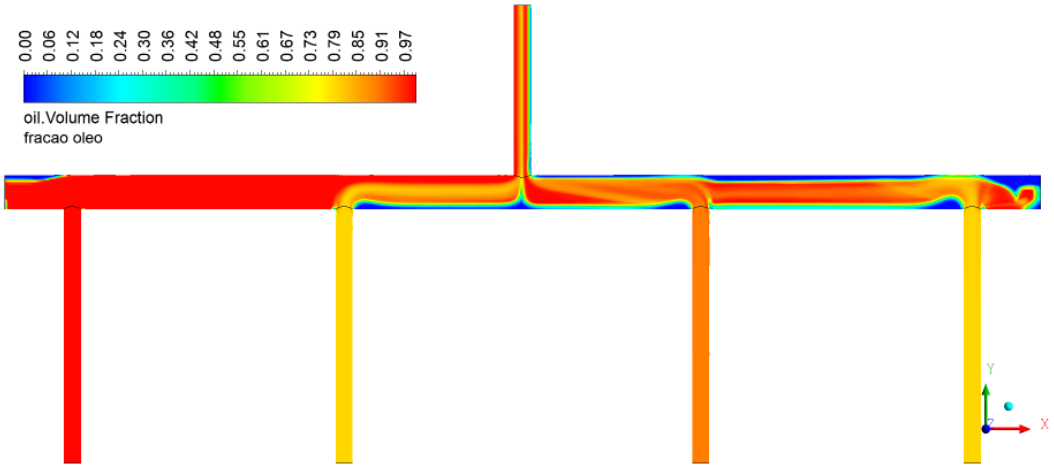

Figure 3. A volumetric fraction of the oil phase (Proposal 1)

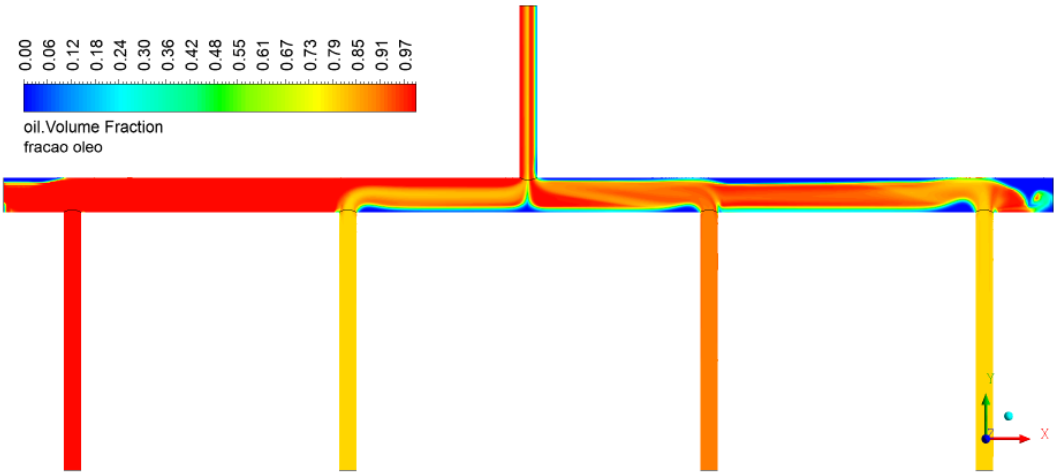

Figure 4. A volumetric fraction of the oil phase (Proposal 2)

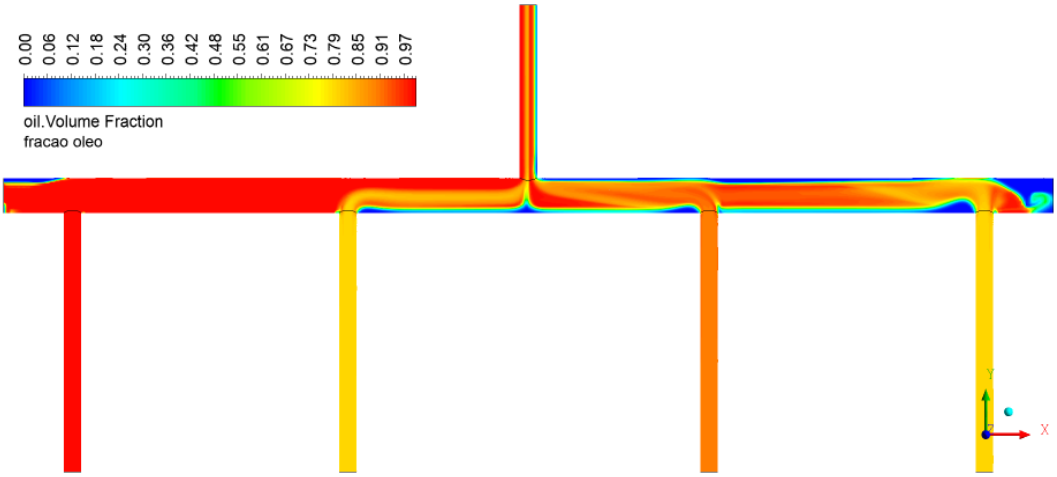

Figure 5. A volumetric fraction of the gas phase (Proposal 3).

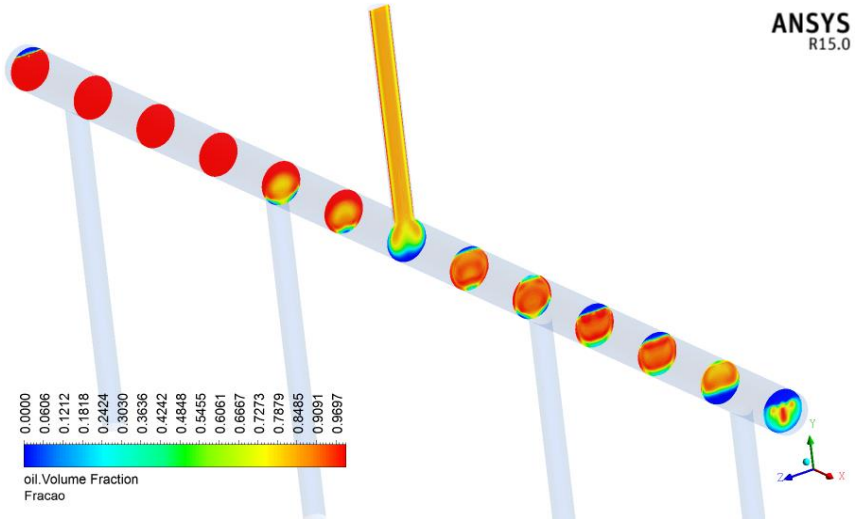

Figure 6. Predominant flow pattern analyzing the oil volumetric fraction (Proposal 1).

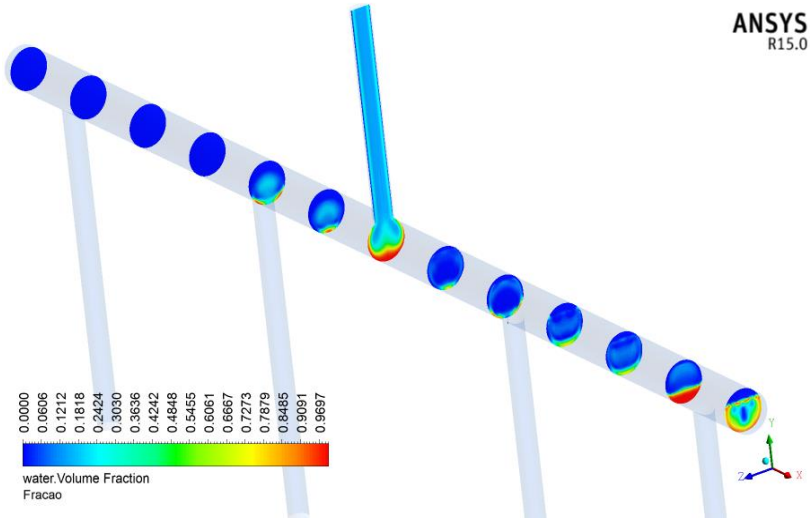

Figure 7. Predominant flow pattern analyzing the water volumetric fraction (Proposal 1).

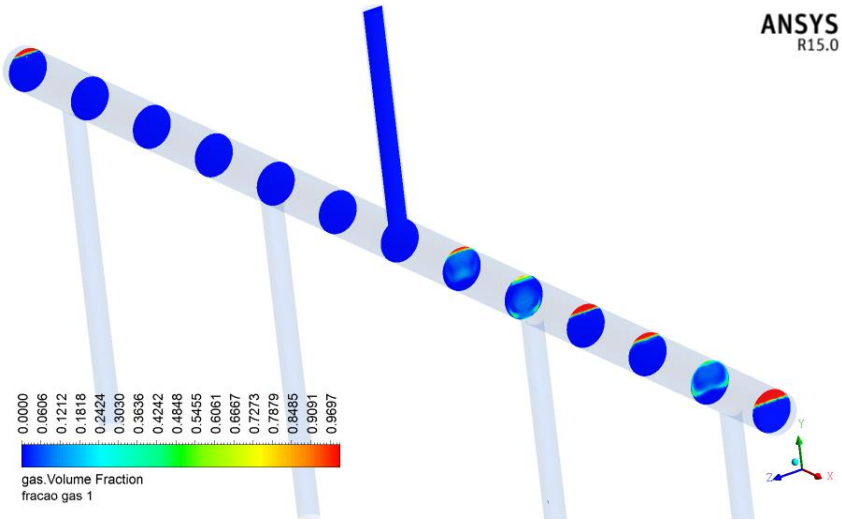

Figure 8. Predominant flow pattern analyzing the gas volumetric fraction (Proposal 1).

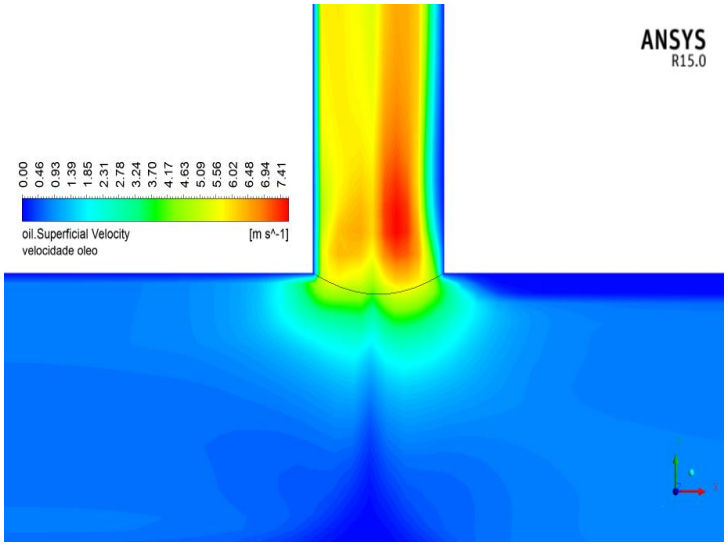

Figure 9. Oil surface velocity (Proposal 1).

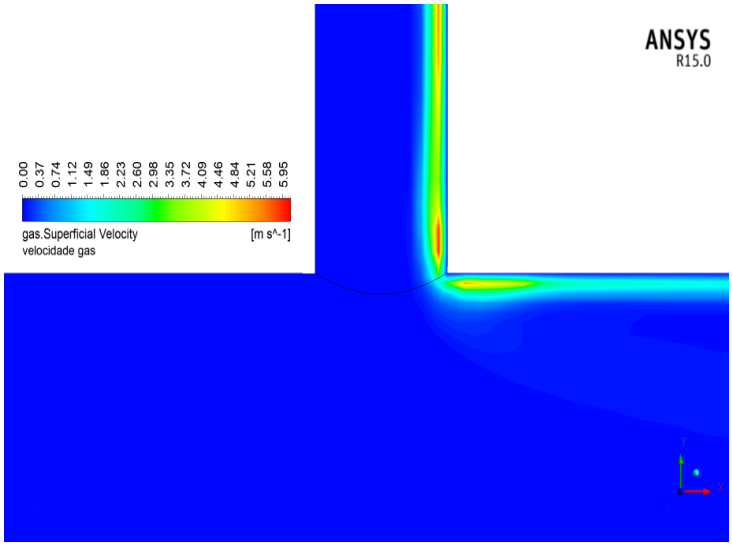

Figure 10. Gas surface velocity (Proposal 1).

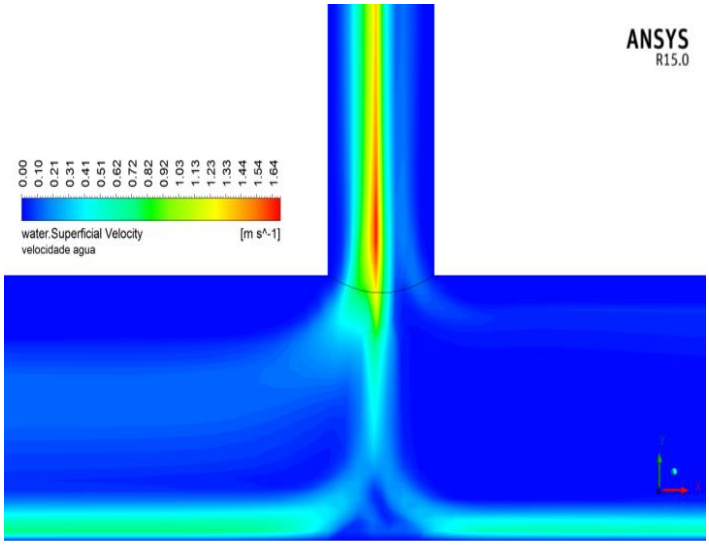

Figure 11. Water surface velocity (Proposal 1).

4. CONCLUSIONS

Based on numerical results obtained in the simulations of three-phase flow (water-oil-gas) in a manifold, it can be concluded that there were no significant changes in the velocity field and the flow regimes for the three proposals presented. However, the goal of minimizing water production was achieved, obtaining an output stream with only 7% of water.

5. ACKNOWLEDGEMENTS

The authors are grateful for the financial support of the government agencies CNPq and CAPES for this research.

6. REFERENCES

Alves, H. G; Magalhães, H. L. F; Santos, W. R. G; Araújo, M. V; Lima, A. G. B; Farias Neto, S. R. “Modelagem e Simulação do Processo de Mistura não Isotérmica em Junção T”, In Congresso Brasileiro de Engenharia Química, COBEQ 2016. Fortaleza, Brasil.

Araújo, M. V; Luna, F. D. T; Farias Neto, S. R; Lima, A. G. B. “Simulação numérica da Detecção de Vazamento em Oleoduto Contendo Conexão TÊ”, In: Congresso Brasileiro de Engenharia Química, Florianópolis, Brasil, 2014.

Barbosa, E. S. “Aspectos Geométricos e Hidrodinâmica de um Hidrociclone no Processo de Separação de Sistemas Multifásicos: Aplicação na Indústria de Petróleo”, Thesis, Universidade Federal de Campina Grande, Campina Grande, Brasil 2011.

Oliveira, M. F. D. Análise da aplicação de um sistema de bombeamento multifásico submarino na produção de petróleo, Dissertation, Pontifícia Universidade Católica do Rio de Janeiro, Rio de Janeiro, 2013.

Silva, F. N; Andrade, T. H. F; Lima, A. G. B; Farias Neto, S. R. “Estudo Numérico do Escoamento Trifásico (Água-Óleo Pesado-Gás) Tipo Core-Flow em uma Conexão T”, In: Congresso Brasileiro de P&D em Petróleo e Gás,PDpetro 2011. Florianópolis, Brasil.

Thomas, J. E., 2001. Fundamentos de Engenharia de Petróleo. Editora interciências, Rio de Janeiro, 1nd.

7. RESPONSIBILITY NOTICE

The authors are the only responsible for the printed material included in this paper.